19th Brazilian Congress of Thermal Sciences and Engineering
November 06th-10th, 2022, Bento Gonçalves - RS - Brazil

ENC-2022-0241

OFFSHORE H_2 PRODUCTION VIA STEAM METHANE REFORMING WITH CARBON CAPTURE

Jade Spinola Ávila
Julio Augusto Mendes da Silva
Fernando Luiz Pellegrini Pessoa
Industrial Engineering Program, Federal University of Bahia, Salvador, Brazil
jade.engavila@gmail.com
jamsilva08@gmail.com
pessoa@eq.ufrj.br
Jislane Santana dos Santos
Post-graduate Program in Chemical Engineering, Federal University of Campina Grande, Campina Grande, Brazil
santosjislane@gmail.com
Ewerton Emmanuel da Silva Calixto
Computational Modeling Department, University Center SENAI CIMATEC, Salvador, Brazil
ewerton.calixto@fieb.org.br
Marcelo da Costa Amaral
Petroleo Brasileiro S.A., R&D Center (CENPES), Rio de Janeiro, Brazil
marceloamaral@petrobras.com.br

Abstract. *The hydrogen from steam methane reforming (SMR) can be supplied on a large scale from the optimization and improvement of existing technologies, being considered a transition route to the green* H_2 *exclusive consumption of the future. The objective of this work is to evaluate the offshore* H_2 *production by SMR method, from an energetic, exergetic and environmental point of view, considering carbon capture by chemical absorption (CA) and supersonic separation (SS). An integrated system involving the processes of* H_2 *production, seawater desalinization, carbon capture and* CO_2 *compression was developed and simulated using Aspen Plus software, which results were verified using data from the literature. From the mass and energy balances, was possible to quantify the thermal and electrical demands of the processes that is supplied by a simplified utility plant. From an energy and exergy viewpoint, the conversion of natural gas to* H_2 *using CA for carbon capture has lower efficiency than adopting SS. When evaluating the energy demand of each process, the CA is responsible for approximately 52% and the SS represents only 24% in relation to energy demand of the entire integrated system. It was observed that the specific energy consumption of the CA is 78% higher than the SS, and the specific exergy consumption of SS is approximately 47% higher than the CA. Therefore, these analyses indicates that the SS technology, in addition to having advantages associated with its modularity and occupy less space favoring its installation on offshore platforms, presents lower energy consumption, and the type of energy required (electrical) is higher quality, presenting a better work potential.*

Keywords: *steam methane reforming, hydrogen production, carbon capture, simulation*

1. INTRODUCTION

The global energy demand is expected to double by 2030, reaching a peak of 80 to 120 million barrels of oil per day (Qyyum et al., 2021), therefore, to mitigate climate change, future energies must be clean (carbon-free), renewable or recyclable (Fu et al., 2021). It is evident that the provision of these energy, free or nearly CO_2 free is a major technological challenge that requires significant advances, government initiatives and industry innovations (Yu et al., 2021). A promising solution to reduce dependence on fossil fuels and meet future demands for sustainable energy is to use H_2 as an energy vector, then its molecule is carbon-free and has a high energy content, being an important pillar in the energy transformation that can contribute to the global warming mitigation (Qyyum et al., 2021). Annually, about 75 million tons of hydrogen are generated worldwide (Adam & Engelshove, 2020), with about 95% of the H_2 production used in refineries in the hydro treatment of fuels to reduce sulfur concentration and as raw material in fertilizer industries and petrochemical plants. However, in the future, an increase in the hydrogen uses as fuel in cars, trucks, ships, and planes, in the process heating and in the electricity generation in turbines is expected.

The hydrogen can be produced from renewable and non-renewable sources, with widely varying costs and CO_2 emissions (Yu et al., 2021), being the production route a determining factor for its environmental feasibility. The hydrogen can be produced by water electrolysis using renewable energy sources, known as green H_2, by steam methane reforming (SMR) from fossil fuels, gray H_2, by SMR associated with carbon capture and storage, blue H_2 (IEA, 2019), by pyrolysis generating solid carbon as a by-product, turquoise H_2 (Silva, 2021), and by extracting hydrogen from bituminous sands and conventional oil fields without CO_2 emissions, H_2 aqua (Yu et al., 2021). Current H_2 production is about 120 million tons per year (IEA, 2019), about 95% of all hydrogen produced in worldwide being generated from natural gas, i.e. SMR (Bakey, 2015), grey H_2. This method has significant CO_2 emissions, 9 - 9.5 $kgCO_2/kgH_2$ (IRENA, 2019; Adam & Engelshove, 2020), generating approximately 830 million tons of CO_2 per year (IEA, 2019). On the other hand, by associating the SMR with a CCS, this factor can be reduced to values around 1.8 $kgCO_2/kgH_2$ (Nanaki & Koroneos, 2017). In this context, carbon capture and storage has shown to be a promising alternative, therefore this CO_2 can be transported to a geological storage site or to oil production wells, where CO_2 injection provides enhanced oil recovery - EOR (Araújo et al., 2017). Uu

A fundamental premise of the hydrogen economy is a low or zero carbon hydrogen supply and a cheap and accessible production route (Yu et al., 2021). The hydrogen produced from fossil fuels is still more economical compared to hydrogen generated by low-carbon technologies (Yu et al., 2021). The hydrogen production cost by SMR is 1,7-2,8 USD/kgH_2 (IEA, 2019), value significantly lower than the one obtained with the water electrolysis and renewable sources, 3,0-7,5 USD/kgH_2 (IEA, 2019). This difference is associated with the high cost of plants and the intermittent power supply, usually resulting in a system underutilization (low-capacity factor). Therefore, for hydrogen to be widely used in the future energy matrix, its production must contain low carbon emissions and be economically viable (Yu et al., 2021).

From the blue H_2 production, characterized by the CO_2 capture, is observed a potential for decarbonization of the energy scenario and compliance of climate goals. It is expected that, in the long term, the investment and production costs of green hydrogen from electrolysis will reduce, due to large-scale applications, better production processes and possible new technologies routes (Adam & Engelshove, 2020). However, in the short and medium term, blue H_2 (low carbon) can be supplied on a large scale from the optimization and improvement of existing technologies, being considered a transition route to the green H_2 exclusive consumption of the future. The offshore integrated process is proposed due to the availability of natural gas as the main raw material and fuel for utilities production, of seawater that is desalinized and subsequently converted into steam and used as cooling water, as well as the proximity of mature wells for storage of the CO_2 captured in the process. In this context, this work aims to evaluate and compare, in terms of energy, exergy and CO_2 emissions, the integrated process of H_2 generation via SMR with carbon capture by chemical absorption and supersonic separation in an offshore scenario.

2. OVERALL PROCESS DESCRIPTION AND METHODS

Figure 1 presents the integration between the plants involved in this work. The hydrogen plant uses natural gas (1) and seawater after desalinization (2), to produce an H_2 - rich stream (4) and generates acid water (3) as a by - product. The carbon capture plant receives the stream rich in H_2 (4) and at the end of the process generates a stream with higher concentration of H_2 (5) and a stream rich in CO_2 (6) which is directed to the compression plant (7). The desalinization plant receives seawater (8) and produces desalinized water (2) and brine (9). Plants can use seawater as a cooling fluid (Cuchivague, 2015) reinforcing the advantage of offshore installation. These processes are supported by heat and electricity generated by the utility plant coupled with the steam reformer. The combustion zone of the reformer is supplied with natural gas (10) and air (11), generating a stream of exhaust gas (12) at high temperature which is used for the steam and electricity production.

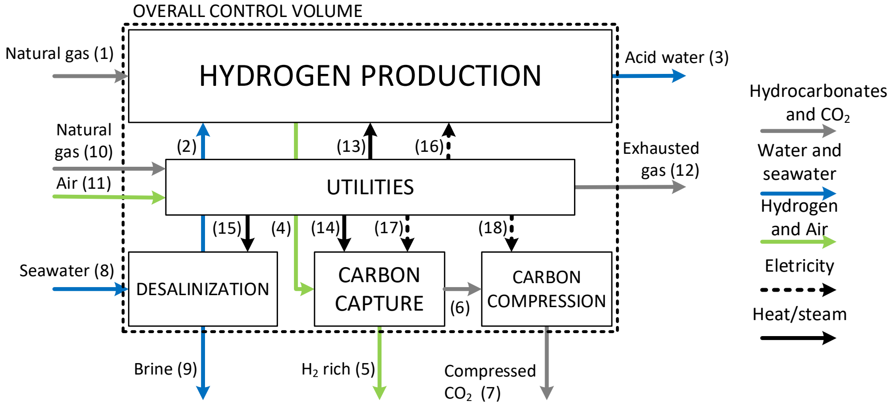

Figure 1 – Overall control volume of the process.

The H_2 production, carbon capture by chemical absorption, desalinization and carbon compression were simulated using Aspen Plus™ software. Unit Operation Extension (UOE) in Aspen Hysys™ was used for the supersonic separation simulation. The UOE is a Visual Studio unit which can be integrated to Aspen Hysys. This UOE was developed in the research project at SENAI CIMATEC with Petrobras. For the simulations, on both software, was used equations of state specific for each case. For the H_2 production, supersonic separation and CO_2 compression plant, the Peng Robinson (PR) equation of state was used due to the presence of hydrocarbons components. For the desalinization and absorption chemical plant, the non-random equation for electrolytes (ELECNRTL) was used due to the presence of solutions and electrolytes.

Hydrogen production. The H_2 production via SMR involves pre-treatment, pre-reforming, reforming and the water gas shift (WGS) steps. In the natural gas pre-treatment, liquid components and sulfur are removed (Molburg & Doctor, 2003). Desulfurization is necessary to avoid sulfur adsorption on the reformer catalyst surface, which can cause a reduction in catalytic activity and a consequent reduction in total plant efficiency (Jakobsen & Åtland, 2016). In this work, it is assumed that natural gas has already gone through the pre-treatment stage on the offshore platform and, therefore, does not have significant amount water or sulfur in its composition. Figure 2 presents the flowchart of the simulated process for H_2 generation.

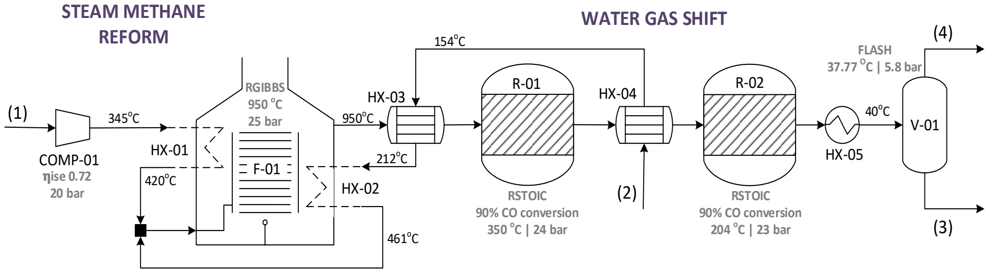

Figure 2 - H_2 generation plant.

Initially, the natural gas pressure and temperature are increased in COMP-01 and HX-01 in order to be mixed with steam. The steam is generated from the water stream coming from the desalinization plant (2) using the heat exchangers (HX-02, HX-03 and HX-04). Due to space constraints on an offshore platform, the pre-reform and reform reactions occurs simultaneously in the reformer. The reformer (F-01) consists of several internal tubes filled with a nickel-based catalyst (Jakobsen & Åtland, 2016), where occurs the conversion of hydrocarbons into carbon monoxide and hydrogen (Molburg & Doctor, 2003), Eq. (1), with a steam to natural gas mass ratio of 3:1 (Al Khusaibi & Rao, 2016; Lira et al., 2018).

$$CH_4 + H_2O \rightarrow CO + 3H_2 \qquad \Delta hr = +\ 206\ kJ/kmolCH_4 \qquad (1)$$

The steam methane reforming concentrates the greatest thermal demand on the plant due to the endothermic reactions that occur in the reformer at temperatures between 500 and 950 ºC (Boyano et al., 2011; Cruz, 2010; Wu & Kuo, 2015; Jakobsen & Åtland, 2016). To represent the reformer, it was assumed a multiphase equilibrium reactor, based on Gibbs free energy. After the reform, the gas stream rich in CO, H_2 and H_2O, known as synthesis gas, is directed to the water gas shift step, characterized by the CO conversion into H_2 by an exothermic reaction, Eq. (2). This step is composed of two reactors (Song et al., 2015). The first reactor (R-02), at 350 ºC, has a higher reaction velocity (Molburg & Doctor, 2003), and the second reactor (R-03), at 204 ºC, increases the equilibrium concentration of the product, since the reaction is exothermic (Fan et al., 2016). For the simulation of the reactor - Eq. (2), a stoichiometric reactor was used based on the reaction conversion fraction, in this case a fixed conversion of 90% was considered according to Molburg & Doctor (2003).

$$CO + H_2O \leftrightarrow CO_2 + H_2 \qquad \Delta hr = -\ 41.2\ MJ/kmolCO \qquad (2)$$

After the water gas shift step, the H_2 rich stream is sent to a flash type separator (V-01), where the liquid and gas phases are separated (Jakobsen & Åtland, 2016). The liquid phase has hydrocarbons traces, i.e. acid water (3) while the gaseous stream (4) is sent to the carbon capture plant.

Carbon capture. Gas separation technologies are used to achieve the required specifications of a particular gas, which consists mainly of CO_2 removal, the most common technologies being: absorption, adsorption, membrane permeation and supersonic separation (Cao & Bian, 2019), where the absorption, adsorption and membrane permeation are already widely applied and commercially mature (Medeiros et al., 2017).

Although Chemical Absorption (CA) presents economic and environmental disadvantages in relation to solvent loss, high energy demand and equipment corrosion, this technology has an excellent performance in terms of solubility and selectivity (Barbosa, 2018). In the CO_2 absorption process, monoethanolamine (MEA), diethanolamine (DEA) and methyl diethanolamine (MDEA) are the ethanolamines commonly used (Marin et al., 2016). In Brazilian refineries, almost all gas treatment, fluidized catalytic cracking and hydrotreating units operates with amines. In Hydrogen Generating Units, the MEA is used to purify the synthesis gas by CA, instead of physical adsorption, to obtain greater purity (Martins, 2011). The carbon capture used in this work consists of an absorption column followed by a regeneration column. The process flowchart and simulation specifications are shown in Fig. 3. In the absorption column, the gas stream (4) enters through the base of the column and the recycled solvent, MEA, enters through the top, forming a counter-current flow in the absorber. The solvent flow required for capture was 12 times (mass) the inlet gas flow at 40 °C and 1 bar with 20% (by mass) of MEA. The H_2 rich gas exits at the absorber top (5), while the CO_2 captured by the solvent leaves the absorber base and goes to the regeneration column. The regeneration performance is very sensitive to the boiler temperature, which cannot exceed 130 ºC to avoid solvent degradation (Barbosa, 2018). Parameters such as pressure in the columns, distillate rate and reflux ratio in the regeneration column were determined from a sensitivity analysis to obtain 90% of the CO_2 captured and lower reboiler thermal demand. After regeneration, the CO_2 rich stream (6) is sent to the compression train to reach the required pressure for injection, while the regenerated solvent stream is recycled to the absorption column along with the solvent makeup.

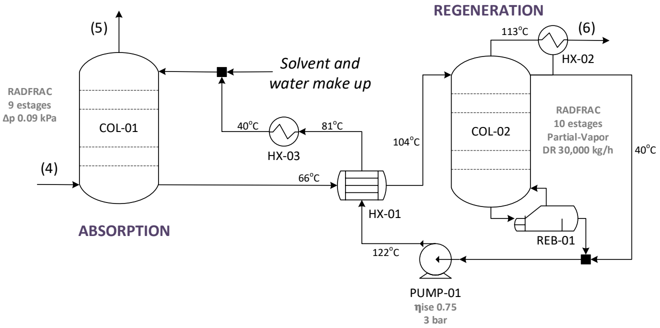

Figure 3 – Chemical absorption plant.

The Supersonic Separation (SS) is capable of condensing and separating water, heavy hydrocarbons, impurities from natural gas and other gases (Cao & Bian, 2019), from the pressure and temperature reduction of the fluid, accelerating it to supersonic speeds in a convergent-divergent nozzle. The SS refers to a combination of a turbo-expander, with a cyclone separator and a compressor for gas recompression (Brouwer et al., 2004), and the equipment efficiency is related to the cooling properties of the convergent-divergent nozzles with the centrifugal separation principles (Haghighi et al., 2015). In the SS, the feeding (4) goes through the converging nozzle, L_C, initiating acceleration/expansion at subsonic speed with Mach < 1 and successive isentropic compressions. Then, the sound speed is reached in the throat with Mach = 1, and goes at the diverging nozzle (L_D) with Mach > 1, characterized by successive isentropic expansions. In the end, there is a H_2 rich gas stream (5) and a CO_2-rich condensate stream (6) which is directed to the compression plant. The Fig. 4 shows a typical representation of a SS. The SS mathematical modeling developed was based, mainly, on Medeiros et al. (2019), book with several approach about natural gas processing with SS and other publications like Alnoush & Castier (2019) and, with regard the sound speed calculation, was used the procedure presented by Castier (2011).

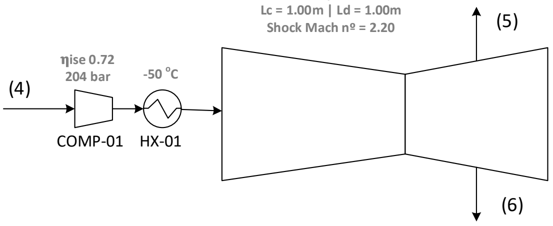

Figure 4 – Supersonic separation plant.

Desalinization. The main commercial desalinization technologies are membrane separation and distillation. Membrane separation (reverse osmosis) methods use pressure gradients across a semi-permeable membrane to filter out unwanted minerals. Distillation occurs due to changes in seawater pressure and temperature, which promote evaporation and subsequent water condensation (Hogerwaard et al., 2019), this method is considered to provide the highest quality, thus requiring less post-treatment for demineralization and avoid incrustation (Meier, 2014). The seawater desalinization by multiple effects is the most suitable alternative for steam production on large scale due to the use of residual heat between the evaporators. This method is characterized by the water and salts separation by a sequency of evaporators (Dastgerdi et al., 2016). The configuration of eight evaporators was adopted. The seawater (8) is distributed equally between the evaporators, the first stage operates at 57.7 ºC and 0.17 bar and the last one at 40 ºC and 0.07 bar, with the other stages operating in intermediate conditions (Hamad et al., 2018). The products of this process are pure water stream (2) and a brine stream (9).

CO_2 compression. The CO_2 injection reduces the viscosity and density of the oil due to the miscibility between them, improving fluidity and increasing the oil recovery factor (R. de P. F. Silva, 2018), thus it is being considered one of the methods for enhanced oil recovery - EOR. This strategy aims to increase well productivity and useful life, recover additional oil and mitigate climate change by reducing CO_2 emissions (Eide et al., 2019). The injection pressure depends on the depth and geological characteristics of the well. In the case presented by Araújo et al. (2017), for example, it is considered 300 bar, while Silva et al. (2020) used 450 bar as pressure required for injection. The compression system is characterized by compression stages followed by a heat exchanger (intercooler) and a separation vessel to remove condensed gases. Thus, it is possible to avoid excessive temperature rise while reducing the work required. A compression train with three compressors in series was modeled. The CO_2 rich gaseous stream that leaves the CO_2 capture plant (6) feeds the compression system, generating a high-pressure CO_2 stream (7). A polytropic efficiency of 75% and an intercooling temperature of 40 ºC were assumed.

Utilities plant. The energy demand for H_2 production, carbon capture, CO_2 compression and desalinization plants is supplied by the combustion that occurs in the reformer reactor of the H_2 plant. According to Fig. 7, natural gas (10) is combusted in the air presence (11) in the combustion section (at 1500oC and 18 bar) to provide heat for the reforming reaction in the radiation section and also for the heat exchangers, HX - 01 and HX - 02, in the convection section (F. E. Da Cruz, 2010). After the reform, the combustion gas from the reformer still at moderate pressure and high temperature is used to supply electricity by expansion (16, 17 and 18) and to generate high (14) and medium (15) pressure steam.

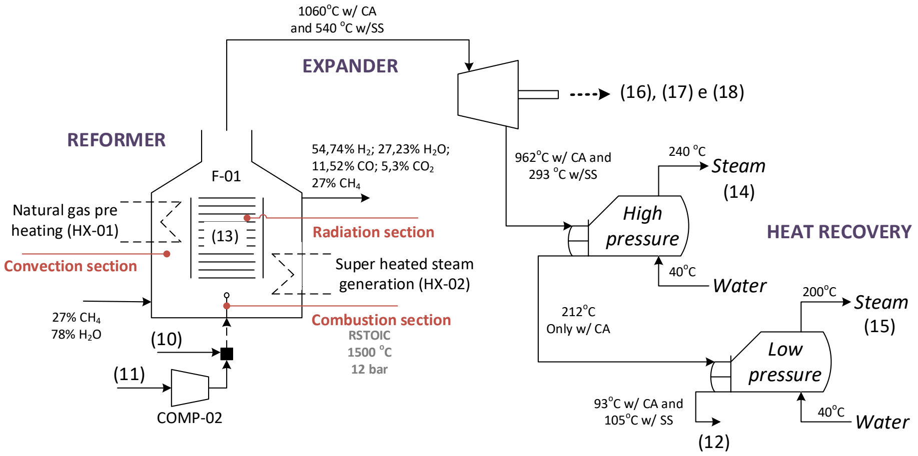

Figure 5 – Utilities plant

3. PERFORMANCE INDICATORS

The indicators adopted are the CO2 specific emission, the energy and exergy efficiencies and, the specific consume of energy and exergy in relation to H2 produced from each carbon capture processes. Initially, to determine the performance indicators, it is necessary to calculate the currents energy (MJ/kg) by Eq. (3). Where the LHV is the low heating value and the Δh represents the enthalpy variation between the analyzed temperature and the lower calorific value reference temperature. The emission factor indicator (gCO_2/MJ) considers the carbon that was emitted to the atmosphere during the evaluated processes, Eq. (4), and the lower calorific value of the hydrogen rich stream produced, Eq. (5).

$$\text{Energy} \quad (e) \quad = \quad \text{LHV} \quad + \quad \Delta h \tag{3}$$

$$m\_CO_{2\ \text{Emitted}} = m\_CO_{2\ \text{Combustion}} + m\_CO_{2\ \text{Reform}} - m\_CO_{2\ \text{Captured}} \tag{4}$$

$$\text{Emission Factor} = [m\_CO_{2\text{Emitted}} / (m\_H_{2\text{Rich}} \text{ x } e\_H_{2\text{Rich}})] \text{ x } 1.000 \tag{5}$$

The energy efficiency was evaluated considering the ratio between the natural gas used and hydrogen rich stream produced energy, Eq. (6).

$$\eta\text{Energy (\%)} = (\text{m\_H}_{2\text{Rich}}\text{ x e\_H}_{2\text{Rich}})/\ (\text{m\_NG x e\_NG}) \tag{6}$$

Exergy is the capacity a given substance has to produce work. The stream total exergy (MJ/kg) is determined by Eq. (7) and the physical and chemical exergies are calculated by Eq. (8) and (9) respectively. Therefore, from the total exergy of the currents it is possible to calculate the exergy efficiency of the integrated processes, Eq. (10).

$$\text{Exergy (b)} = b_{ph} + b_{ch} \tag{7}$$

$$b_{ph} = \Delta h - T_o\,(s - s_o) + (V^2/2) + gz \tag{8}$$

$$b_{ch} = \sum y_i e_{chi} + RT_o \sum y_i \ln y_i \tag{9}$$

$$\eta\text{Exergy (\%)} = (\text{m\_H}_{2\text{Rich}}\text{ x b\_H}_{2\,\text{Rich}})/\ (\text{m\_NG x b\_NG}) \tag{10}$$

To determine energy, Eq 11, and exergy, Eq 12, specific consume, the utility consumption of the CA and SS processes are considered in terms of energy (e_CarbonCapture) and exergy (b_CarbonCapture) in relation to H_2 rich stream generated by both processes.

$$\text{Specific Energy}^{\text{CA/SS}} = \text{e\_CarbonCapture/ m\_ H}_{2\text{Rich}} \tag{11}$$

$$\text{Specific Exergy}^{\text{CA/SS}} = \text{b\_CarbonCapture/ m\_ H}_{2\text{Rich}} \tag{12}$$

4. RESULTS AND DISCUSSIONS

Table 1 lists the characteristics of the streams indicated in Fig. (1).

Table 1 - Streams thermodynamic properties.

	Mass flow rate (kg/s)	Temperature (°C)	Pressure (bar)	Composition (mol)
1	1.25	21.11	5.00	$0.95CH_4$; $0.007CO_2$; $0.016N_2$; 0.028HCs
2	3.63	40.00	2.00	1.00 H_2O
3	1.00	38.00	2.00	$0.9999H_2O$; $0.0001CO_2$
4	3.88	38.00	2.00	$0.008CH_4$; $0.78H_2$; $0.009H_2O$; $0.19CO_2$; $0.003N_2$; 0.001CO;
5^{CA}	0.72	25.00	3.00	$0.01CH_4$; $0.9732H_2$; $0.01H_2O$; $0.004N_2$; 0.001CO;
5^{SS}	0.82	-79.45	47.33	$0.0099CH_4$; $0.9765H_2$; $0.0037N_2$; $0.0087CO_2$;
6^{CA}	2.08	20.00	2.00	$0.012H_2O$; $0.988CO_2$
6^{SS}	3,06	-66.20	47.33	$0.0005CH_4$; $0.0010H_2$; $0.0447H_2O$; $0.9537CO_2$; $0.001N_2$
7^{CA}	2.08	16.73	450.00	$0.012H_2O$; $0.988CO_2$
7^{SS}	3.11	16.73	450.00	$0.0005CH_4$; $0.0010H_2$; $0.0447H_2O$; $0.9537CO_2$; $0.001N_2$
8	9.17	37.00	1.00	0.98 H_2O; 0.01Na+; 0.01Cl-
9	5.53	40.00	0.07	0.96 H_2O; 0.02Na+; 0.02Cl-
10^{CA}	1.67	21.11	5.00	$0.95CH_4$; $0.007CO_2$; $0.016N_2$; 0.028HCs
10^{SS}	0.97	21.11	5.00	$0.95CH_4$; $0.007CO_2$; $0.016N_2$; 0.028HCs
11^{CA}	37.50	25.00	1.00	$0.21O_2$; $0.79N_2$
11^{SS}	18.75	25.00	1.00	$0.21O_2$; $0.79N_2$
12^{CA}	39.44	92.61	0.70	$0.0007CH_4$; $0.15H_2O$; $0.07CO_2$; $0.04O_2$; $0.72N_2$; 0.002HCs
12^{SS}	19.72	92.61	0.70	$0.0007CH_4$; $0.15H_2O$; $0.07CO_2$; $0.04O_2$; $0.72N_2$; 0.002HCs

CA: Chemical Absorption; SS: Supersonic Separation;

Based on the thermal and electrical demand required for the processes, the temperature and pressure in the reformer were selected as 1500 °C and 12 bar. Table 2 presents the thermal and electrical demand and the equipment in which they are generated. Steam 1 is at 200 °C and 2 bar and steam 2 is at 240 °C and 5 bar, and the electrical demand related to the pumps and compressors consumption in the subsystems.

Table 2 – Thermal and electrical demand.

Stream	Energy (kW)	Power source
13	25,271.93	Reformer burning gas (HX-01; HX-02; F-01)
14^{CA}	36,529.54	Steam 2 (REB-01); Steam 1 (HX-01)
15	1,400.00	Steam 1 (EV-01)
16	186.74	Expander
17^{CA}	7.87	Expander
17^{SS}	10,163.77	Expander
18^{CA}	1,330.50	Expander
18^{SS}	1,187.35	Expander

Steam Methane Reforming. The global result indicates an energy efficiency to the CH_4 conversion into H_2 of 81.74%. This value is higher than those indicated in the literature, Table 3, due to the reform temperature used on the references. In case presented by Jakobsen & Åtland (2016) was used a reform temperature (850 ºC), by Molburg & Doctor (2003) the temperature was 815 ºC, Boyano et al. (2011) operated at 700 ºC and Cruz (2008) used 840 ºC, both temperatures lower than the simulated in this work (950 ºC). From these data, is verified that the conversion is directly proportional to the temperature of the reforming reactor. Another important point is the energy supplied presented by Cruz (2008), like the used in this work (2.5 item).

Table 3 - Steam methane reforming plant specific consumption.

Indicators	Al Khusaibi & Rao (2016)	Jakobsen & Åtland (2016)	Molburg & Doctor (2003)	Boyano et al. (2011)	Cruz (2008)	Simulated
Rich H_2 produced per NG consumed (kg_{H2}/kg_{GN})	0.32	0.27	0.38	0.38	0.25	0.45
Steam consumed per Rich H_2 produced (kg_{H2O}/kg_{H2})	-	0.81	1.09	1.21	-	0.93
Thermal energy required per rich H_2 produced (kJ_t/kg_{H2})	$22.9x10^3$	$40.9x10^3$	-	$37.3x10^3$	-	$44.11x10^3$
Electrical energy required per rich H_2 produced (kJ_e/kg_{H2})	-	-	-	-	-	48.05
Process Efficiency (%)	-	82.00	75.16	70.43	81.70	81.74

Chemical Absorption. As presented in Table 4, the deviations are due to different operating conditions: (i) (R. de P. F. Silva, 2018) simulated the CO_2 capture from a gas with 5.78% CO_2 (mol) using 50% solvent (by mass) of MDEA and PZ; (ii) (Martins, 2011) simulated the CO_2 capture from a gas with 24.48% CO_2 (mol) using 20% (by mass) of MEA. In this work was used MEA solvent 20% (by mass) to capture carbon from a gas stream with 19% CO_2 (mol).

Table 4 - Chemical absorption plant specific consumption.

Indicators	Martins (2011)	Silva (2018)	Simulated
Demand solvent per H_2 rich ($kg_{Solvent}/kg_{Gas}{}^a$)	24.20	15.00	13.95
Demand solvent per captured CO_2 ($kg_{Solvent}/kg_{Top}{}^b$)	27.50	21.07	25.97
Thermal demand per regeneration distillate rate ($kJ_t/kg_{DR}{}^c$)	$4.3x10^3$	$1.8x10^3$	$3.5x10^3$

[a] Absorber column inlet gas stream; [b] Regenerating column gas stream from top; [c] Regenerating column distillate rate.

Supersonic separation. The SS is considered a new technology in the context of H_2 production, therefore, there was a difficulty in finding data for supersonic separation of a gas stream from methane steam reforming so far. The mathematical modeling used to develop the supersonic separation was verified using the data obtained in the literature. The parameters necessary for the simulation, like a geometry data (Di, Do, Lc and Ld), separator input stream conditions (P and T) and shock Mach number were determined from tests using an initial guess based in the literature until convergence and better separation performance between the H_2 and CO_2. Furthermore, the target was a H_2 (5) and CO_2 (6) purity in the gas stream higher than these generated stream by CA. In this way, from the simulation results it was possible to observe that there was a good separation of components, the H_2 was concentrated in the gas stream and the water and CO_2 were condensed, achieving the desired objective. Table 5 presents data from the supersonic separation collected in the literature and those obtained in the simulation. The main difference between the simulated cases is the fluid composition at the separator input. The gas stream of Arina (2004) is composed of air and in the other references it is composed of CH_4, heavy hydrocarbons and CO_2. Arina (2004) presented a similar geometry, this fact can be explained due to the similar gas composition (no heavy hydrocarbons).

Table 5 – Supersonic separation results.

Parameters	Arina (2004)	Wen et al. (2012)	Arinelli et al. (2017)	Simulated
Converging Angle (°)	4.943	23.06	22.39	5.515
Diverging Angle (°)	2.65	4.72	2.26	5.52
Inlet Mach	0.156	0.0403	0.0509	0.0014
Throat Area (m^2)	0.0001	0.0011	0.0012	0.0001
Shock Pressure (bar)	27.58	17.90	11.60	20.60
Shock Temperature (°C)	-74.709	-105.78	-52.69	-113.42

Desalinization. Table 6 shows the results found on the literature to the desalinization plant. Hamad et al. (2018) and Guimard et al. (2019), use a thermal steam compressor that improves the process and consumes lower thermal energy, in this work this technology was not considered. Elsayed et al. (2018) simulated with 12 evaporators and obtained higher indicator based on used seawater per purified water than the desalinization plant simulated, that was used 8 evaporators. Other differences such as the salinity of the water also contribute for the discrepancies found in the result.

Table 6 - Desalinization plant specific consumption.

Indicators	Hamad et al. (2018)	Guimard et al. (2019)	Dong et al. (2019)	Elsayed et al. (2018)	Simulated
Used seawater per purified water ($kg_{seawater}/kg_{water}$)	2.62	-	2.45	2.94	2.52
Produced brine per purified water (kg_{brine}/kg_{water})	1.62	2.02	1.45	1.95	1.52
Salt concentration in brine (kg_{salt}/kg_{brine})	0.058	-	-	0.07	0.065
Thermal demand per purified water (kJ_t/kg_{water})	252.00	252.00	-	-	360.00

Carbon Compression. Regarding the CO_2 compression, Table 7 indicates the results found in the literature which are dependent of pressure variation. In case presented by Cuchivague (2015), the compression evaluated used two compression trains (four stage each) with a pressure variation of 249 bar, while in Rodrigues (2013) the pressure variation was 567 bar and three compression stages were used. For Silva (2018), the pressure variation was 449 bar and 3 stages were considered.

Table 7 - Carbon compression specific consumption.

Indicators	Cuchivague (2015)	Rodrigues (2013)	Silva (2018)	Simulated
Electrical demand per CO_2 compressed and pressure variation ($kJ_e/kg_{CO2}.bar$)	1.00	1.00	0.90	1.00

4.1 Global Indicators

According to global indicators obtained, the carbon capture plant by CA captures 66% of the CO_2 entering the absorber column, thus the CO_2 emission factor obtained is 6.46 $kgCO_2/kgH_2$, being 32% lower than the emission factor for a SMR plant without carbon capture (9.5 $kgCO_2/kgH_2$). By using the supersonic separation was possible to capture 80% of CO_2 and the CO_2 emission factor is 3.89 $kgCO_2/kgH_2$, representing 40% lower than in the conventional (CA) process. When evaluating the energy demand of each process, the CA is responsible for approximately 52% of the energy demand of the entire integrated system and the SS represents only 24%. This fact is associated with the energy type required in this process, while the CA uses thermal (REB-01 and HX-01) and electrical energy (COMP-01), the SS uses only electrical energy (COMP-01) due to the compression in the begin and along the supersonic.

In order to develop the comparison of the processes energy type independently, the utilities are evaluated in exergy terms, according to the specific consumptions in Table 8. It was observed that the specific energy consumption of the CA is 78% higher than the SS, since the CA is supplied by a large thermal energy load. From the exergy point of view, the specific exergy consumption of SS is approximately 47% higher, since the exergy portion contained in the steam stream that supplies the CA is lower than the exergy contained in the electric power. From an energy viewpoint, the conversion of natural gas to H_2 using CA for carbon capture has 21.35% lower efficiency than adopting SS as presented in Table 9. Regarding exergy, which considers the chemical potential of the fuel stream used as feedstock and the hydrogen generated, the exergy efficiency obtained with CA is ~32% lower than with SS. Thus, the thermal demand reduction using SS, generating almost the same flow of product (H_2), is reflected in increased energy and exergy efficiency for the overall process. Emissions from methane direct use (57.31 gCO_2/MJ_{NG}) are almost the same than from hydrogen produced offshore via SMR with carbon capture by CA and ~42% higher than from SS. Therefore, these analyses indicates that the SS technology, in addition to having advantages associated with its modularity, presents lower energy consumption, and the type of energy required (electrical) is higher quality, presenting a better work potential.

Table 8 – Calculated indicators for the integrated system with chemical absorption and supersonic separation.

Indicators	CA	SS
Energy demand per H_2 rich (kJ/kg)	15.72	3.44
Exergy demand per H_2 rich (kJ/kg)	1.82	3.44
η Emission (gCO_2/MJ)	56.44	33.57
η Energy (%)	53.25	77.87
η Exergy (%)	25.60	37.51

5. CONCLUSIONS AND FUTURE WORKS PROPOSAL

In the short and medium term, blue H_2 can be supplied on a large scale from the optimization and improvement of existing technologies, being considered a transition route to the green H_2 exclusive consumption of the future. In this context, this work discusses the performance of offshore hydrogen production via SMR in energy and exergy efficiency and CO_2 emission terms with carbon capture by CA and SS. The global performance indicators were obtained considering the control volume that involves H_2 generation, desalinization, carbon capture, CO_2 compression and utilities plants. When evaluating the energy demand of each process, the CA is responsible for approximately 52% of the energy demand of the entire integrated system and the SS represents only 24%. From an energy and exergy viewpoint, the conversion of natural gas to H_2 using CA for carbon capture has lower efficiency than adopting SS. According to obtained carbon capture plant indicators, the carbon capture plant by CA captures 66% of the CO_2 entering the absorber column, and using the SS was possible to capture 80% of CO_2. It was observed that the specific energy consumption of the CA is 78% higher than the SS, since the CA is supplied, mainly, by a large thermal energy load. In relation to exergy, the specific exergy consumption of SS is approximately 47% higher, since the exergy portion contained in the steam stream that supplies the CA is lower than the exergy contained in the electric power. Therefore, these analyses indicates that the SS technology, in addition to having advantages associated with its modularity and occupy less space favoring its installation on offshore platforms, presents lower energy consumption, and the type of energy required (electrical) is higher quality, presenting a better work potential. Considering the necessity to evaluate the H_2 purification process to expand the possibilities of its application and increase its added value, is possible to evaluate the gas purification of the gas also by SS. Thus, a series SS plant is proposed contemplating the CO_2 capture and contaminants removal. Within the offshore H_2 production context, there are opportunities for research developments associated with the gas transport assessment. Two scenarios can be evaluated: i) offshore – transport of the produced H_2 to the coast; ii) onshore – transport of natural gas to the coast and CO_2 back to the platform to be injected into mature wells.

References

Adam, P., & Engelshove, S. (2020). Hydrogen infrastructure – the pillar of energy transition gas networks to hydrogen operation. *Whitepaper Siemens*, 32.

Al Khusaibi, S., & Rao, L. N. (2016). Design and Production of Hydrogen Gas by Steam Methane Reforming Process - A Theoretical Approach. *International Journal of Science Technology & Engineering*, *3*(01), 472–476. http://www.ijste.org/articles/IJSTEV3I1128.pdf

Alnoush, W., & Castier, M. (2019). Shortcut modeling of natural gas supersonic separation. *Journal of Natural Gas Science and Engineering*, *65*(February), 284–300. https://doi.org/10.1016/j.jngse.2019.03.004

Araújo, O. de Q. F., Reis, A. de C., de Medeiros, J. L., Nascimento, J. F. do, Grava, W. M., & Musse, A. P. S. (2017). Comparative analysis of separation technologies for processing carbon dioxide rich natural gas in ultra-deepwater oil fields. *Journal of Cleaner Production*, *155*, 12–22. https://doi.org/10.1016/j.jclepro.2016.06.073

Bakey, K. (2015). *The Production of Hydrogen Gas: Steam Methane Reforming*. http://sites.psu.edu/kevinbakey/wp-content/uploads/sites/26382/2015/04/Process-Description.pdf

Barbosa, L. C. (2018). *Analysis of technologies for separation of CO2 in offshore platforms: Physical absorption by ionic liquids, chemical absorption by amines and permeation by membranes*. UFRJ.

Boyano, A., Blanco-Marigorta, A. M., Morosuk, T., & Tsatsaronis, G. (2011). Exergoenvironmental analysis of a steam methane reforming process for hydrogen production. *Energy*, *36*(4), 2202–2214. https://doi.org/10.1016/j.energy.2010.05.020

Cao, X., & Bian, J. (2019). Supersonic separation technology for natural gas processing: A review. *Chemical Engineering and Processing - Process Intensification*, *136*, 138–151. https://doi.org/10.1016/j.cep.2019.01.007

Castier, M. (2011). Thermodynamic speed of sound in multiphase systems. *Fluid Phase Equilibria*, *306*(2), 204–211.

Cruz, F. E. Da. (2010). Hydrogen Production in Oil Refineries: Exergetic Evaluation and Production Cost Hydrogen Production in Oil Refineries: Exergetic Evaluation and Production Cost. In *Dissertação de Mestrado*. USP.

Cruz, F., & De Oliveira, S. (2008). Petroleum refinery hydrogen production unit: Exergy and production cost evaluation. *International Journal of Thermodynamics*, *11*(4), 187–193.

Cuchivague, H. Y. O. (2015). *Análise exergética de um sistema de injeção de CO2 para uma plataforma FPSO e sua integração com Ciclo Combinado e Captura de Carbono.* (Issue Ic). Universidade Estadual de Campinas.

Dastgerdi, H. R., Whittaker, P. B., & Chua, H. T. (2016). New MED based desalination process for low grade waste heat. *Desalination*, *395*, 57–71. https://doi.org/10.1016/j.desal.2016.05.022

de Medeiros, J. L., Arinelli, L. de O., & Araújo, O. de Q. F. (2017). Speed of sound of multiphase and multi-reactive equilibrium streams: A numerical approach for natural gas applications. *Journal of Natural Gas Science and Engineering*, *46*, 222.

de Medeiros, J. L., de Oliveira Arinelli, L., Teixeira, A. M., & Araújo, O. de Q. F. (2019). Offshore Processing of CO2-Rich Natural Gas with Supersonic Separator. In *Offshore Processing of CO2-Rich Natural Gas with Supersonic Separator*.

Dong, Z., Liu, M., Huang, X., Zhang, Y., Zhang, Z., & Dong, Y. (2019). Dynamical modeling and simulation analysis of a nuclear desalination plant based on the MED-TVC process Reactor Core. *Desalination*, *456*(May 2018), 121–135.

Eide, L. I., Batum, M., Dixon, T., Elamin, Z., Graue, A., Hagen, S., Hovorka, S., Nazarian, B., Nøkleby, P. H., Olsen, G. I., Ringrose, P., Augusto, R., & Vieira, M. (2019). *(CO 2) Infrastructure Developments — A Review*. *1*, 1–21.

Elsayed, M. L., Mesalhy, O., Mohammed, R. H., & Chow, L. C. (2018). *Transient performance of MED processes with di ff erent feed con fi gurations*. *438*(February), 37–53. https://doi.org/10.1016/j.desal.2018.03.016

Fan, J., Zhu, L., Jiang, P., Li, L., & Liu, H. (2016). Comparative exergy analysis of chemical looping combustion thermally coupled and conventional steam methane reforming for hydrogen production. *Journal of Cleaner Production*, *131*, 247.

Fu, Q., Wang, D., Li, X., Yang, Q., Xu, Q., Ni, B. J., Wang, Q., & Liu, X. (2021). Towards hydrogen production from waste activated sludge: Principles, challenges and perspectives. *Renewable and Sustainable Energy Reviews*, *135*(August 2020).

Guimard, L., Cipollina, A., Ortega-delgado, B., Micale, G., Couenne, F., Bandelier, P., & Jallut, C. (2019). New considerations for modelling a MED-TVC plant under dynamic conditions. *Desalination*, *452*(November 2018), 94–113.

Haghighi, M., Hawboldt, K. A., & Abedinzadegan Abdi, M. (2015). Supersonic gas separators: Review of latest developments. *Journal of Natural Gas Science and Engineering*, *27*, 109–121. https://doi.org/10.1016/j.jngse.2015.08.049

Hamad, M. Ben, Ruiz-Femenia, R., Snoussi, A., Brahim, A. Ben, & Caballero, J. (2018). *Minimizing the total annualized cost of " SIDEM " seawater desalination unit*. *115*, 22467. https://doi.org/10.5004/dwt.2018.22467

IEA, I. E. A. (2019). The Future of Hydrogen. In *The Future of Hydrogen* (Issue June). https://doi.org/10.1787/1e0514c4-en

IRENA, I. R. E. A. (2019). *Hydrogen: A renewable energy perspective* (Issue September).

Jakobsen, D., & Åtland, V. (2016). Concepts for Large Scale Hydrogen Production [Norwegian University of Science and Technology]. In *Master Thesis*. https://brage.bibsys.no/xmlui/handle/11250/2402554

Lira, R. L. T. C., Lima, N. M., & Lucena, S. (2018). Simulation of the production of industrial hydrogen and synthesis gas via natural gas using ASPEN HYSYS software. *Revista de Química Industrial*, 53–61.

Marin, M. P. A. ., Ferreira, N. L. ., Queiroz, A. P. ., Fortini, P. L. A., & Tacacima, J. . (2016). ESTUDO DO PROCESSO DE CAPTURA DO CO 2 PROVENIENTE DOS FUMOS DA QUEIMA DO GÁS NATURAL EM CALDEIRAS. *XXI Congresso Brasileiro de Engenharia Química*.

Martins, P. R. L. (2011). *Evaluation of the CO2 absorption process with amines using HYSYS*. UFRJ.

Meier, K. (2014). Hydrogen production with sea water electrolysis using Norwegian offshore wind energy potentials. *Int J Energy Environ Eng*, *5*(104). https://doi.org/10.1007/s40095-014-0104-6

Molburg, J. C., & Doctor, R. D. (2003). Hydrogen from Steam-Methane Reforming with CO2 Capture. *20th Annual International Pittsburgh Coal Conference*, 21.

Nanaki, E. A., & Koroneos, C. J. (2017). Exergetic aspects of hydrogen energy systems-The case study of a fuel cell bus. *Sustainability (Switzerland)*, *9*(2). https://doi.org/10.3390/su9020276

Qyyum, M. A., Dickson, R., Ali Shah, S. F., Niaz, H., Khan, A., Liu, J. J., & Lee, M. (2021). Availability, versatility, and viability of feedstocks for hydrogen production: Product space perspective. *Renewable and Sustainable Energy Reviews*, *145*(September 2020), 110843. https://doi.org/10.1016/j.rser.2021.110843

Rodrigues, L. C. (2013). *Evaluation of scenarios for the recovery of natural gas liquids and CO2 injection in the context of the pre-salt layer*. Federal University of Rio de Janeiro.

Silva, F. C. N., Freire, R. L. A., Orrego, D. F., & Oliveira, S. de; (2020). Comparative assessment of advanced power generation and carbon sequestration plants on offshore petroleum platforms. *Energy*, *203*. https://doi.org/10.1016/j.energy.2020.117737

Silva, R. de P. F. (2018). *Avaliação de Sistemas Termelétricos e de Captura e Sequestro de Carbono em Processamento Offshore de Gás Natural Rico em CO2*. Universidade Federal do Rio de Janeiro.

Song, C., Liu, Q., Ji, N., Kansha, Y., & Tsutsumi, A. (2015). *Optimization of steam methane reforming coupled with pressure swing adsorption hydrogen production process by heat integration*. *154*, 392–401.

Wu, W., & Kuo, P. C. (2015). Conceptual designs of hydrogen production, purification, compression and carbon dioxide capture. *Energy Conversion and Management*, *103*, 73–81. https://doi.org/10.1016/j.enconman.2015.06.046

Yu, M., Wang, K., & Vredenburg, H. (2021). Insights into low-carbon hydrogen production methods: Green, blue and aqua hydrogen. *International Journal of Hydrogen Energy*, *46*(41), 21261–21273.

Silva. B. (2021). Do cinzento ao turquesa. quanto custa produzir cada tipo de hidrogénio? Economia online.